MOLECULAR AND CELLULAR BIOLOGY, July 2009, p. 3633–3643 Vol. 29, No. 13
0270-7306/09/$08.00+0 doi:10.1128/MCB.00362-09


# ZNF536, a Novel Zinc Finger Protein Specifically Expressed in the Brain, Negatively Regulates Neuron Differentiation by Repressing Retinoic Acid-Induced Gene Transcription▽

Zhen Qin,[1] Fangli Ren,[1] Xialian Xu,[1] Yongming Ren,[1] Hongge Li,[2] Yinyin Wang,[1] Yonggong Zhai,[3] and Zhijie Chang[1]*

*School of Medicine, Department of Biological Sciences and Biotechnology, State Key Laboratory of Biomembrane and Membrane Biotechnology, Tsinghua University, Beijing, China[1]; Northwest Plateau Institute of Biology, Chinese Academy of Sciences, Xining, and Graduate University of Chinese Academy of Sciences, Beijing, China[2]; and College of Life Science, Beijing Normal University, Beijing, China[3]*

Received 20 March 2009/Accepted 20 April 2009

**Neuronal differentiation is tightly regulated by a variety of factors. In a search for neuron-specific genes, we identified a highly conserved novel zinc finger protein, ZNF536. We observed that ZNF536 is most abundant in the brain and, in particular, is expressed in the developing central nervous system and dorsal root ganglia and localized in the cerebral cortex, hippocampus, and hypothalamic area. During neuronal differentiation of P19 cells induced by retinoic acid (RA), ZNF536 expression is increased at an early stage, and it is maintained at a constant level in later stages. Overexpression of ZNF536 results in an inhibition of RA-induced neuronal differentiation, while depletion or mutation of the ZNF536 gene results in an enhancement of differentiation. We further demonstrated that ZNF536 inhibits expression of neuron-specific marker genes, possibly through the inhibition of RA response element-mediated transcriptional activity, as overexpression of RA receptor α can rescue the inhibitory role of ZNF536 in neuronal differentiation and neuron-specific gene expression. Our studies have identified a novel zinc finger protein that negatively regulates neuron differentiation.**

Transcription factors play pivotal roles in directing the formation of neurons and gliacytes in the mammalian nervous system. All neurons, astrocytes, and oligodendrocytes in the adult nervous system originate ultimately from progenitor cells located in the ventricular zone of the embryonic neural tube (38). The generation of new neurons is a complicated process which involves a number of tightly coordinated steps, including the commitment of multipotent stem cells to a neuronal (rather than glial) fate, arrest of progenitor divisions, acquisition of differentiated features by postmitotic precursors, growth of axons and dendrites, and migration of the nascent neurons out of the germinal zone toward a particular laminar position in the cortical plate (11). Important progress has been made to date in the characterization of regulatory mechanisms during these steps. Many transcription factors have been shown to regulate aspects of neurogenesis and to play a central role in the neurogenic process. For instance, transcription factors *Pax6* and *Ngn1*/*Ngn2* are two proneural factors and are actively involved in determining transmitter phenotypes (9, 29). Furthermore, several intracellular factors have been shown to play critical roles in postnatal neurogenesis. TLX, an orphan nuclear receptor, and Bmi-1 are intracellular factors required for the maintenance of adult forebrain neuron stem cells (21, 27, 31). Another intracellular factor, DISC1, controls dendritic growth and physiological maturation in newborn dentate granule cells (8).

Zinc finger proteins are an important class of eukaryotic DNA-binding proteins and play a critical role in the development and differentiation of the nervous system. Zinc finger proteins have an evolutionarily conserved structure which defines a large family of transcription factors (35). One of the zinc finger proteins is the retinoic acid receptor (RAR), which is classified as a Cys4 zinc finger nuclear receptor belonging to the hormone receptor superfamily and is found in the central nervous system, including the hippocampus and cortex. RAR deficiency in mice virtually eliminates long-term potentiation in hippocampal CA1 and results in deficits of spatial learning and memory tasks (36). Another type of zinc finger proteins has the Cys2His2 motif. Kruppel-like zinc finger transcription factors contain this motif and have been implicated in the regulation of the development of the nervous system. For instance, the Zic zinc-finger transcription factors have been shown to play essential roles in regulating the proliferation and differentiation of neuronal progenitors in the medial forebrain and cerebellum. The Zic Zic1, Zic2, and Zic3 genes are expressed by progenitor cells in the septum and cortical hem, the sites of generation of the Cajal-Retzius cells, and regulate the proliferation of meningeal cells and pial basement membrane assembly (12). The Ikaros (Ik) zinc finger transcription factors function in the hypothalamic-pituitary axis. Ik-1 and Ik-2 proteins act as positive regulators of ENK gene expression in the developing striatum. Ik is also involved in the maturation and differentiation of striatal medium spiny neurons (14).

Retinoic acid (RA) has been proven to be involved in neuronal patterning, neural differentiation, and axon outgrowth. Recent data highlight the roles of RA in introducing specific neuronal cell types for therapeutic transplantation and in regenerating axons after damage. In addition, RA is involved in

* Corresponding author. Mailing address: School of Medicine, Department of Biological Sciences and Biotechnology, Tsinghua University, Beijing (100084), China. Phone: (86-10) 62785076. Fax: (86-10) 62773624. E-mail: zhijiec@tsinghua.edu.cn.

▽ Published ahead of print on 27 April 2009.

the maintenance of the differentiated state of adult neurons and neural stem cells, and altered RA signaling levels lead to the appearance of symptoms of several neurodegenerative diseases (18). The essential role of RA in neuronal differentiation has been extensively studied by in vitro models using embryonal carcinoma (EC) cells and neuroblastoma cells (13, 28). RA induces the differentiation of various types of neurons and gliacytes by activating the transcription of many genes encoding transcription factors, cell signaling molecules, structural proteins, enzymes, and cell surface receptors (19). Binding of RA to RARs (which bind several forms of RA) and retinoid X receptors (RXRs) (which bind only 9-*cis*-RA) induces a conformational change in the receptors, altering the balance between coactivator and corepressor interactions, and allows a switch from repression to activation of target gene expression (3, 4, 10). The receptors form both homo- and heterodimers to interact with bipartite DNA binding sites, the RA response elements (RAREs), or the retinoid response elements (24).

In this study, we identified a novel zinc finger protein, ZNF536, that is most abundant in neuronal cells of the brain and spinal cord. Interestingly, we observed that exogenous expression of ZNF536 inhibits all-*trans*-RA-induced P19 EC cell differentiation and that depletion of ZNF536 promotes cell differentiation into neuronal cell types. We found that ZNF536 negatively regulates RA-induced gene transcription by binding to RAREs and interrupting RA receptor α (RARα) binding.

## MATERIALS AND METHODS

**Plasmids and reagents.** The KIAA0390 clone containing the full-length human ZNF536 coding sequence was kindly provided by Takahiro Nagase, KAZUSA DNA Research Institute, Chiba, Japan. The pEGFP-N1/Flag-ZNF536 plasmid was constructed with the KIAA0390 clone by using a PCR-based strategy. The C-terminal binding protein (CtBP)-binding motif deletion plasmid pEGFP-N1/Flag-ZNF536mu was constructed by applying a PCR-based strategy using a Takara MutanBEST kit, according to information on a predicted typical CtBP-binding motif, PLDLSVP (5). The construct for establishing G418-resistant knockdown cell lines was subcloned from ZNF536 small interfering RNA (siRNA) double-stranded oligonucleotide into pSilencer 4.1/cytomegalovirus vector. pRARE-Luc reporter and human RARα1 expression construct plasmids were kindly provided by Wen Xie, University of Pittsburgh. All-*trans*-RA was purchased from Sigma. Anti-ZNF536 rabbit polyclonal antibodies were generated by immunizing rabbits with purified glutathione *S*-transferase-ZNF536 (97 to 475 amino acids) fusion protein and were affinity purified by an antigen-coupled Sepharose column in this laboratory. Anti-Flag M2 monoclonal antibody, anti-β-actin monoclonal antibody, anti-β-tubulin III monoclonal antibody, and anti-glial fibrillary acidic protein (anti-GFAP) monoclonal antibody were purchased from Sigma. Anti-RARα polyclonal antibody and anti-green fluorescent protein (anti-GFP) polyclonal antibody were purchased from Santa Cruz Biotechnology. Fluorescent secondary antibodies (goat anti-rabbit immunoglobulin G [IgG] and goat anti-mouse IgG) were purchased from Jackson ImmunoResearch Laboratories. The horseradish peroxidase-conjugated secondary antibodies for enhanced chemiluminescence were purchased from Pierce. Flag-ZNF217 was expressed by a vector, pMT3-Flag-hZNF217, kindly provided by Merlin Crossley (23).

**Cell culture, differentiation, and generation of stable cells.** Human embryonic kidney 293T and murine EC P19 cells were maintained in Dulbecco's modified Eagle's medium (DMEM) supplemented with 10% heat-inactivated fetal bovine serum and 100 units/ml penicillin-streptomycin. For induction of neuronal differentiation, $1 \times 10^5$ cells/ml of P19 cells in DMEM were treated with 0.3 μM all-*trans*-RA and plated using bacterial-grade dishes. After 4 days of culture in suspension in the presence of RA, P19 cells formed embryonic body stages (EBs). EBs were collected from suspension cultures and then plated by using a tissue culture surface without RA. To establish stable cell lines expressing wild-type ZNF536, mutant ZNF536, and siRNA, expression plasmids were transfected into P19 cells, which were selected in culture medium containing 500 μg/ml G418. To establish stable cell lines expressing RARα and ZNF536, the RARα1 expression plasmid and the pHygro vector were cotransfected into ZNF536 stable overexpression cell lines by selection with culture medium containing 500 μg/ml G418 and 300 μg/ml hygromycin. Resistant cells were then further expanded in 10-cm culture dishes and subsequently confirmed by reverse transcription-PCR (RT-PCR) analysis.

TABLE 1. Primers used in real-time RT-PCR

| Gene and primer type | Primer sequence |
|---|---|
| 18s rRNA | |
| Forward | 5′-GAGAAACGGCTACCACATCC-3′ |
| Reverse | 5′-CCTCCAATGGATCCTCGTTA-3′ |
| β-Actin | |
| Forward | 5′-TCGTCGACAACGGCTCCGGCATGT-3′ |
| Reverse | 5′-CCAGCCAGGTCCAGACGCAGGAT-3′ |
| mZNF536 | |
| Forward | 5′-GAGTTCCGCTGTGAGGTATGT-3′ |
| Reverse | 5′-GGGATTTGTTCTTCACCGATA-3′ |
| hZNF536 | |
| Forward | 5′-AAGCGAAACGCAAAGATAACA-3′ |
| Reverse | 5′-TGCCTGGGTAAACACCAAACT-3′ |
| Pax6 | |
| Forward | 5′-TGCCCTTCCATCTTTGCTTG-3′ |
| Reverse | 5′-TCTGCCCGTTCAACATCCTTAG-3′ |
| MAP2 | |
| Forward | 5′-CTGTAACCCTGTCTTAGTGCC-3′ |
| Reverse | 5′-TGAACCAACATCTGTAAACCC-3′ |
| β-Tubulin III | |
| Forward | 5′-TCAGCAAGGTGCGTGAGGAGT-3′ |
| Reverse | 5′-GGTGCGGAAGCAGATGTCGTA-3′ |
| RARα | |
| Forward | 5′-CCTGAGCAAGACACAATGACC-3′ |
| Reverse | 5′-CAGCATCTTGGGGAACATGTG-3′ |
| hRARα | |
| Forward | 5′-GGCTTTTCTCTGCCTTTCTACCGACC-3′ |
| Reverse | 5′-AGGGGCCTCACTCAGTTCCTGGCCT-3′ |

**WM-ISH.** The ZNF536 in situ hybridization probe consisted of a 524-bp fragment (3,199 to 3,723 bp from the coding sequence [CDS] of the ZNF536 gene), which was subcloned into pBluescript KS(−) vector and labeled with digoxigen. For the mice used in the experiments, the morning when the vaginal plug was detected was defined as embryonic day 0 (E0). Whole-mount in situ hybridization (WM-ISH) was performed with the embryos according to the protocol previously described (6).

**RNA isolation, Northern blotting, and real-time RT-PCR.** Total RNA from different tissues from adult mice or cell lines was extracted using TRIzol reagent (Invitrogen). Total RNA (10 μg) from adult mouse tissues were fractionated on a 1% formaldehyde agarose gel and transferred to a nitrocellulose membrane for Northern blotting (37). A ZNF536 probe (3,196 to 4,026 bp from the CDS of the ZNF536 gene) was labeled with $^{32}P$ using a Prime-a-Gene kit (Promega). RNA isolated from cells treated with DNase I (Takara Bio) was used for reverse transcription with SuperScript II reverse transcriptase (Invitrogen) with a random hexamer primer (Promega). The resulting cDNA was used for PCR or quantitative real-time PCR analyses (SYBR green; Applied Biosystems). Primer sequences are listed in Table 1.

**Western blotting.** Cells from cultured cell lines and tissues were lysed in 1 ml cell lysis buffer (80 mM KCl, 10 mM $Na_2HPO_4$, 1 mM EDTA [pH 8.0], 0.5% NP-40, 10% glycerol, 1 mM dithiothreitol, 0.1 mM $Na_3VO_4$, 1 mM phenylmethylsulfonyl fluoride, 1 μg/ml leupeptin, 1 μg/ml pepstatin). Western blot analysis was performed as previously described (17).

**Immunohistochemical analysis.** Mouse brain tissues were collected, and the paraffin-embedded specimens were fixed on glass slides for immunohistochemical analysis. Rabbit anti-ZNF536 antibody or mouse anti-β-tubulin III antibody at a dilution of 1:500 and mouse anti-GFAP antibody at a dilution of 1:200 were used and detected with an immunohistochemistry polymer double detection kit (ZhongShan Golden Bridge Bio, China) according to the manufacturer's protocol.

**Immunofluorescence staining and confocal microscopy.** Slides with mouse brain tissue samples were prepared by following a standard protocol for antigen retrieval and fixing. Cells growing on glass coverslips in six-well clusters were washed with phosphate-buffered saline (PBS), fixed for 30 min at room temperature with 4% paraformaldehyde in PBS, and permeabilized for 10 min with 0.3% Triton X-100 in PBS. Cells were blocked with 10% fetal bovine serum for 45 min at room temperature. Primary antibodies diluted in PBS containing 0.1% Tween 20 were incubated for 2 h at room temperature, and bound antibodies

TABLE 2. Probes used in EMSAs[a]

| Oligonucleotide | Sequence[a] |
|---|---|
| DR-5 | 5′-tcgaGGGTAGGGTTCACCGAAAGTTCACT CGCT-3′ |
| DR5-Mu | 5′-tcgaGGGTAGGGAACACCGAAAGAACACT CGCT-3′ |
| α2RARE | 5′-tcgaCAGGCGAGTTCAGCAAGAGTTCAGC CGAAT-3′ |
| α2RARE-M1 | 5′-tcgaCAGGCGAGTAGTGCAAGAGTAGCGC CGAAT-3′ |
| M67/SIE | 5′-agctTCATTTCCCGTAAATCCCTAAAGCT-3′ |
| APRE | 5′-GCGCCTTCTGGGAATTCCTA-3′ |
| SP1 | 5′-ATTCGATCGGGGCGGGGCGAGC-3′ |

[a] Lowercase type indicates the protection alkali base.

were detected with fluorescein isothiocyanate- or tetramethyl rhodamine isocyanate-conjugated goat anti-rabbit or anti-mouse IgG. Coverslips were mounted in a glycerol-based antifade mounting medium and analyzed with a laser scanning confocal microscopy with a 60× oil immersion objective.

**Luciferase assay.** Luciferase assays were done with the indicated plasmid mixtures using P19 cells as previously described (17) with a reporter vector, pRARE-luc. Cells were treated with RA ($3 \times 10^{-8}$ M) 4 h posttransfection or left untreated for 24 h. The RARE luciferase activity was measured using a luciferase assay system (Promega). The results were expressed as means with standard deviations (SD) from three independent experiments. Data were normalized with *Renilla reniformis* luciferase activity by cotransfection of pTK-RL (Promega) as an internal control.

**Electrophoretic mobility shift assay (EMSA).** Nuclear extracts from P19 stable cell lines were prepared after cells were stimulated with 0.3 μM RA for 24 h or left untreated. Nuclear extracts from 293T cells transiently transfected with the expression plasmids indicated in Fig. 6 were prepared after 24 h of transfection. Nuclear extracts containing the same amounts of total protein were subjected to an electrophoretic mobility shift assay with a $^{32}$P-labeled high-affinity direct repeat 5 (DR-5), a mutant DR-5 (30), and a specific RARE from the mouse RARα2 promoter (α2RARE) probe (16). Competitions were done in the presence of unlabeled 100-fold high-affinity DR-5, mutant DR-5, SP1, α2RARE, mutant α2RARE, and acute-phase response element (APRE) and SIE/M67 oligonucleotides (34). For the supershift assay, reaction mixtures were preincubated with 1 μg of anti-ZNF536 antibody, anti-RARα antibody, or antihemagglutinin (anti-HA) antibody. Mobility shift reactions were resolved on 5% nondenatured polyacrylamide gels. Gels were dried and visualized by using a PhosphorImager. Oligonucleotide sequences are listed in Table 2.

**ChIP.** 293T cells expressing Flag-ZNF536 and RARα for 24 h were used for chromatin immunoprecipitation assays (ChIP). Rabbit IgG antibody, anti-ZNF antibodies, and anti-RARα antibody were used for precipitation, and the precipitants were resolved according to the protocol of the manufacturer (Upstate Biotechnology). The primers for amplifying the precipitated DNA of human RARβ2 promoter were 5′-TCCTGGGAGTTGGTGATGTCAG-3′ (sense) and 5′-AAACCCTGCTCGGATCGCTC-3′ (antisense). PCR was done with annealing at 50°C for 30 s and 40 reaction cycles.

## RESULTS

**Identification and sequence information for *Znf536*.** In order to identify novel factors interacting with CtBP1 (a corepressor for gene transcription), we performed a yeast two-hybrid screening with a mouse brain library (data not shown). Since many clones were obtained, we selected the one with specific expression in the brain. A novel zinc finger protein, ZNF536 (GenBank accession nos. AB002388 for human and AK030633 for mouse), was finally identified. The human *ZNF536* cDNA spans 4,935 nucleotides, encoding a 1,300-amino-acid-long protein. The mouse *Znf536* cDNA spans 4,413 nucleotides encoding a protein of 1,302 amino acids. The identity between the human and mouse sequences is 76% at the nucleotide level and 88% at the amino acid level.

Homology searches identified orthologous genes in the rat, dog, chicken, and zebrafish with very high levels of similarity (86% or greater) in the amino acid sequences of the zinc finger region. All of these genes encode proteins with 10 zinc fingers and a CtBP-binding motif (5) (Fig. 1A). Most of the 10 zinc fingers are of the Kruppel-like zinc finger type (7). A genome-wide search for similar proteins suggested a phylogenetic relationship among five zinc finger protein subfamilies (Fig. 1B), indicating that ZNF536 is most closely related to ZNF219, a protein containing nine zinc fingers that is a transcriptional repressor (25, 26). Taken together, these data indicate that *ZNF536* is highly conserved in vertebrates and represents a new subfamily of zinc finger proteins.

**Expression pattern of *Znf536*.** To determine the function of ZNF536, we first studied the expression pattern of the gene. WM-ISH experiments with mouse embryos aged from E9.5 to E12.5 showed that *Znf536* is expressed in the developing central nervous system, dorsal root ganglia (DRG), eye vesicles, and limbs (Fig. 2A). In particular, *Znf536* is expressed in the developing forebrain, midbrain, hindbrain neural folds, and spinal cord at E9.5 (Fig. 2A, b and c). When the embryo developed to E10.5, we observed that *Znf536* is expressed in the telencephalic vesicles, midbrain, hindbrain, and spinal cord and is detectable in the DRG region and somites (Fig. 2A, e and f). Similar expression patterns were observed at E11.5 and E12.5, with significant expression in the telencephalic vesicles, midbrain, hindbrain, and spinal cord (Fig. 2A, h, i, k, and l). Outside of the central nervous system, *Znf536* is expressed in DRG, forelimb buds, and eye vesicles (Fig. 2A, k and l).

A Northern blot experiment demonstrated that in adult mouse tissues, *Znf536* appears to be expressed predominantly in the brain, while a weak signal was also detected in the heart and testis; however, no expression in the liver, spleen, lung, kidney or stomach was observed (Fig. 2B). It appears that four different transcripts exist in the mouse brain.

Both the WM-ISH and Northern blot experiments consistently indicated that *Znf536* is expressed predominantly in the brain, both in developing mouse embryos and in the adult mouse. A semiquantitative RT-PCR analysis was further performed to demonstrate that *Znf536* mRNA is abundant in the cerebral cortex, hippocampus, thalamus, and corpus striatum of the rat brain (Fig. 2C).

**ZNF536 is expressed in neuronal cells in the adult mouse brain.** To identify the expression pattern of ZNF536 in specific cells, we attempted to perform an immunohistochemical staining experiment with mouse brain sections. We generated anti-ZNF536 polyclonal antibodies. A Western blot analysis indicated that the anti-ZNF536 antibodies specifically recognize the ZNF536 protein (Fig. 3A). The antibodies clearly detected the endogenous ZNF536 protein in P19 cells and mouse brains but not in mouse lung tissue (Fig. 3B). Our immunohistochemistry results demonstrated that the ZNF536 protein is abundant in the cerebral cortex, hippocampus, and hypothalamic area (Fig. 3Ca and b). The expression of ZNF536 in the cerebral cortex and hippocampus (Fig. 3Cc and d) appears to be in neuronal cells, as indicated by the neuronal marker protein β-tubulin III (Fig. 3Ce and f), and not in glial cells, as indicated by GFAP (Fig. 3Cg and h). When ZNF536 and β-tubulin III were double stained using 3,3′-diaminobenzidine tetrahydrochloride (DAB) and alkaline phosphatase (AP) (Fig. 3Ci and

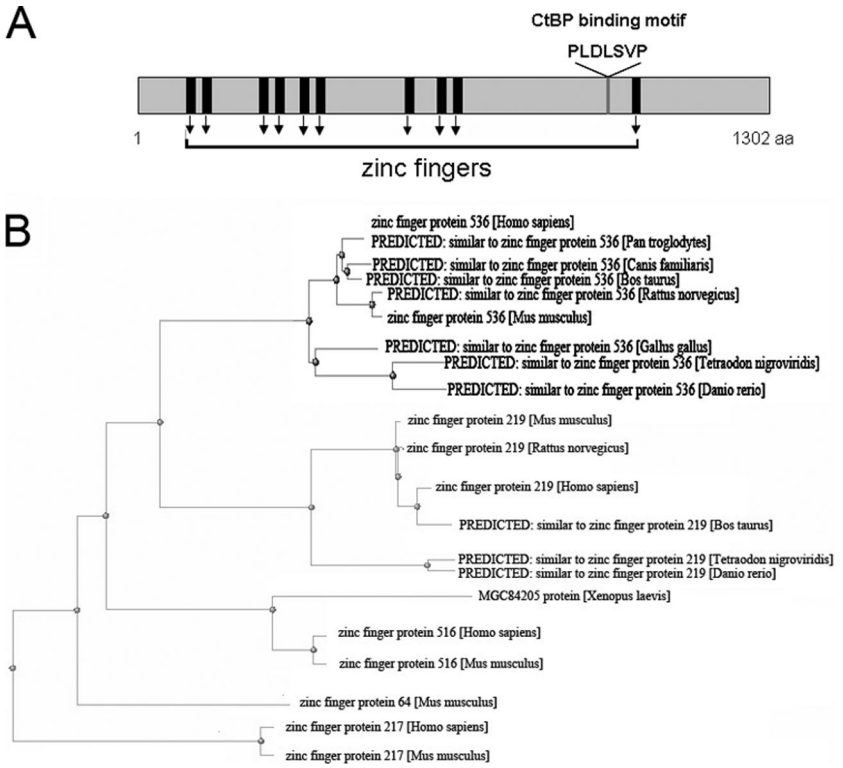


FIG. 1. Sequence information for *Znf536*. (A) A schematic of the structure of Znf536 is shown. Solid boxes refer to the locations of the 10 zinc finger domains; the location of the CtBP motif is shown in red, with the sequence above it. (B) Phylogenetic relationship suggested for ZNF536-related zinc finger proteins generated by BLAST. aa, amino acids.

j), coexpression of ZNF536 and β-tubulin III in the same neuronal cells was observed. Double staining with ZNF536 and GFAP failed to be observed with any cells (Fig. 3Ck and l).

Fluorescence staining experiments clearly indicated that the ZNF536 protein is localized to the nucleus of β-tubulin III-positive cells and that cells with ZNF536-positive staining are mostly GFAP negative in the cortex (Fig. 3D). In the hippocampus, GFAP-positive cells have no ZNF536 staining, while the β-tubulin III-positive cells are ZNF536 positive; both ZNF536 and β-tubulin III are only weakly stained in this region (Fig. 3E). Taken together, these results demonstrated that ZNF536 is specifically expressed in neuronal and not glial cells of the brain.

**ZNF536 is involved in RA-induced neuronal differentiation of P19 cells.** Given that ZNF356 is highly and specifically expressed in neuronal cells, we speculated that ZNF536 may play a role in neuronal cell differentiation. In order to elucidate this function, we chose to study the effects of ZNF536 by using P19 cells, an EC cell line that responds to RA for neuronal differentiation (13). We first examined the endogenous mRNA levels of ZNF536 in differentiating P19 cells. When P19 cells are aggregated in the presence of RA, mRNA levels of ZNF536 increase simultaneously with those of β-tubulin III (Fig. 4A, days 1 to 4). Interestingly, ZNF536 mRNA is constantly at a high level in differentiated cells after the suspension period, when mRNA levels of β-tubulin III begin to decrease (Fig. 4A, days 6 to 14). In a coimmunostaining experiment, we observed that ZNF536-positive cell numbers increase with induction by RA (Fig. 4B, compare day 0 to day 6). Significantly, we observed that cells with lower levels of β-tubulin III exhibit higher levels of ZNF536 (Fig. 4B). These results consistently indicate that expression of ZNF536 is closely related to P19 cell differentiation induced by RA.

Next, we stably expressed human wild-type ZNF536, a mutant of ZNF536 with a defect in the CtBP-binding motif, and an siRNA that silences endogenous ZNF536 in P19 cells (Fig. 5A, left, mRNA levels; right, ectopically expressed hZNF536 proteins). Immunostaining demonstrated that almost no neuron-like cells (indicated by β-tubulin III) could be observed when human ZNF536 is ectopically expressed, but many more neuron-like cells were observed when the mutant of ZNF536 is expressed or the endogenous ZNF536 is depleted (Fig. 5B). Real-time RT-PCR analysis indicated that overexpression of ZNF536 dramatically reduces the mRNA levels of the neuronal marker genes *Pax6*, *MAP2*, and β-*Tubulin III* and that depletion of ZNF536 results in an increase in the mRNA levels of these marker genes (Fig. 5C). These data suggest that ZNF536 inhibits neuronal cell differentiation.

**ZNF536 is involved in RARE-mediated gene regulation.** RA-induced differentiation of P19 cells requires the binding of RAR to RARE in the promoters of RA-targeted genes (1, 3). Since ZNF536 inhibits RA-induced neural differentiation, we speculated that ZNF536 might affect the activation of RAR in the initiation of downstream gene transcription. To test this hypothesis, an RA-responsive reporter, *RARE*-Luc, was used to examine the role of ZNF536 on RAR-induced gene expression. The luciferase reporter experiments show that RA stimulates this reporter more than 300-fold; however, when

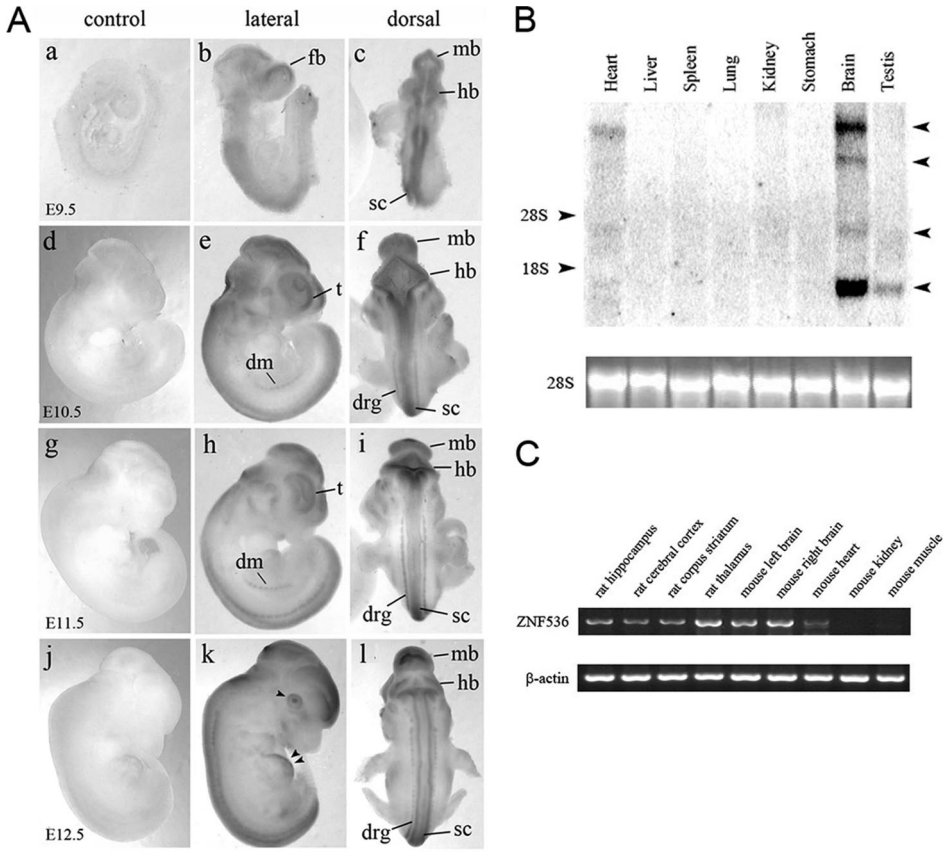


FIG. 2. Expression pattern of *Znf536* in mouse. (A) *Znf536* expression in E9.5 to E12.5 mouse embryos by WM-ISH assays. Parts a, d, g, and j show negative controls using the sense RNA probe. At E9.5 (b and c), *Znf536* was expressed in the forebrain (fb), midbrain (mb), hindbrain (hb) neural folds, and spinal cord (sc). At E10.5 (e and f), *Znf536* transcripts were detected in the telencephalic vesicles (t), midbrain, hindbrain, spinal cord, DRG, and dermomyotomes (dm). At E11.5 (h and i), *Znf536* was detected in the same regions as at E10.5. At E12.5 (k and l), *Znf536* expression was detected in the midbrain, hindbrain, and spinal cord. Outside of the central nervous system, *Znf536* is expressed in the DRG, eye vesicles (k, single arrowhead), and forelimb buds (k, double arrowheads). Lateral (b, e, h, and k) and dorsal (c, f, i, and l) views are shown. (B) Northern blot analysis of *Znf536* in different adult mouse tissues. Four transcripts were detected by using a probe corresponding to consensus CDS sequence. 28S rRNA indicates that equal amounts of total RNA from each tissue were loaded. (C) Expression of *Znf536* in different sections of rat brain and mouse tissues was analyzed by semiquantitative RT-PCR. β-Actin was used as an internal control.

ZNF536 is overexpressed, the response to RA is decreased to 150-fold, suggesting that ZNF536 inhibits RA-induced reporter activity (Fig. 6A, compare the first two columns). To avoid any potential interference with transient transfection in the luciferase assay, we also tested the effect of ZNF536 in stable cell lines. Cells stably expressing ZNF536 reduce RA-induced luciferase activity fourfold (Fig. 6B, compare ZNF wild-type cells to mock-transfected cells), while increased luciferase activity was seen with stable expression of mutant ZNF536 or the siRNA of ZNF536 (Fig. 6B, compare mutant ZNF and ZNF siRNA cells to mock-transfected cells). These data indicate that ZNF536 inhibits RARE-driven gene expression in response to RA stimulation.

The inhibitory role of ZNF536 on RARE-driven gene expression may be generated by a direct association of ZNF536 to RARE in the RA-target gene promoters. To examine this hypothesis, we used a classical RARE (DR-5) and a specific RARE from the mouse RARα2 promoter (α2RARE) as probes for EMSA analysis in the P19 stable cells (Fig. 6C and D, respectively). The results show that RA-treated cells with overexpressed ZNF536 yield increased binding to either the DR-5 or the α2RARE probe (Fig. 6C, compare lane 3 with lane 7; Fig. 6D, compare lane 3 with lane 2). The specificity of RARE binding was confirmed by a supershift assay with the anti-ZNF536 antibodies (Fig. 6D, lane 7) and a competition assay with the specific cold probe (Fig. 6C, lane 4, and Fig. 6D, lane 9); thus, we conclude that ZNF536 associates with RARE. These results imply that ZNF536 represses RARE-driven gene expression by binding to RARE.

Binding of ZNF536 to RARE may also lead to disassociation of the RAR complex from RARE. To test this possibility, we overexpressed RARα together with ZNF536 in 293T cells and used DR-5 as a probe to perform a further experiment using EMSA. The results indicated that two bands occurred (Fig. 6E). The upper band was confirmed to be a RAR complex, since it was diminished in a competition with the anti-RARα antibody (Fig. 6E, lane 2) but not with the anti-ZNF536 antibodies (Fig. 6E, lane 3). The lower band was confirmed to be a ZNF536 complex, since the anti-ZNF536 antibodies blocked the band (Fig. 6E, lanes 3, 7, and 11) but the anti-RARα antibody did not (Fig. 6E, lanes 2, 6, and 10). Significantly, overexpression of ZNF536 enhanced the lower band

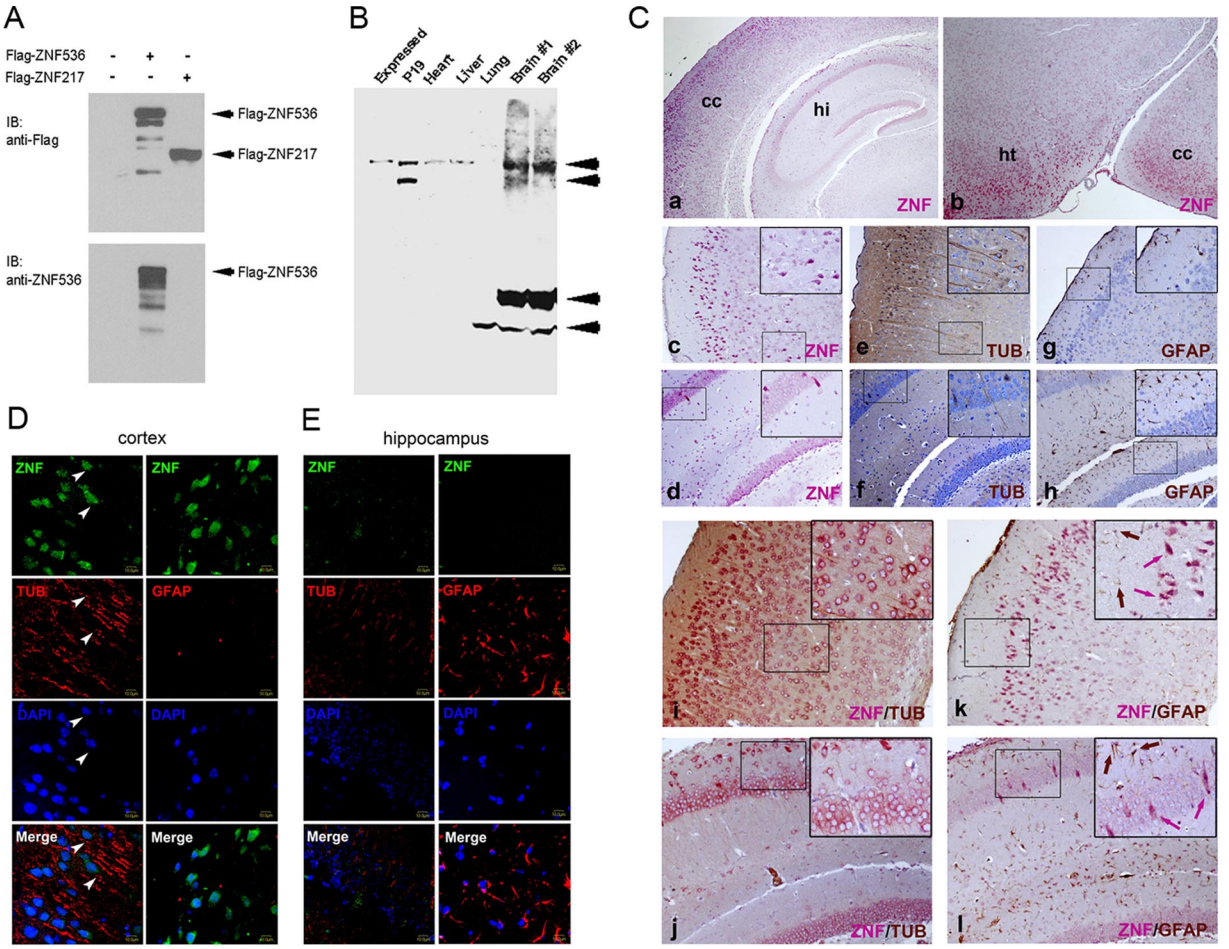


FIG. 3. Distribution of ZNF536 protein in mouse brain sections. (A) A Western immunoblot (IB) presentation of specificity for the anti-ZNF536 antibodies. Flag-ZNF536-GFP was used as a detecting protein for the specificity of the anti-ZNF536 antibodies. A similar protein, Flag-ZNF217, was used as a control. The detection of anti-ZNF536 antibodies is shown in the lower panel. (B) The endogenous ZNF536 protein in the cells and tissues. The endogenous ZNF536 protein levels were examined by using purified antibodies against ZNF536. The total protein from the samples was resolved by 8% sodium dodecyl sulfate-polyacrylamide gel electrophoresis. Brain#1 and brain#2 are from two animals. (C). Representative coronal sections (5 μm) stained by an immunohistochemical for ZNF536 (ZNF) and neuronal related marker proteins. (a to d) Staining of ZNF536 by an AP-Red detection system (magenta). (a) Cerebral cortex (cc) and hippocampus (hi) area (original magnification, 40×). (b) Hypothalamic (ht) area (original magnification, 40×). (c) Cerebral cortex. (d) Hippocampus. (e and f) Staining of β-tubulin III (TUB) by DAB detection system (brown) in cerebral cortex and hippocampus samples, respectively. (g and h) Staining of GFAP by DAB detection system (brown) in cerebral cortex and hippocampus samples, respectively. (i and j) Double staining of ZNF536 (AP-Red) and β-tubulin III (DAB) in cerebral cortex and hippocampus samples, respectively. The coexpression cells show henna staining. (k and l) Double staining of ZNF536 (AP-Red) and GFAP (DAB) in cerebral cortex and hippocampus samples, respectively. Arrows show the different staining of the two antibodies. Nuclei are indicated by hematoxylin staining (blue). The original magnification is 100× except where indicated. An enlarged image is shown at the top right corner of each box. (D to E) ZNF536 localizes to the neuronal cells as indicated by neuronal marker proteins. Mouse brain sections were double labeled with a rabbit anti-ZNF536 antibody (ZNF, green) and a mouse anti-β-tubulin III (TUB, red) or an anti-GFAP antibody (GFAP, red) and stained by immunofluorescence. (D) Cerebral cortex. (E) Hippocampus. Arrows indicate the same cells labeled by both anti-ZNF536 antibody and anti-β-tubulin III. DAPI, 4′,6-diamidino-2-phenylindole. Scale bars, 10 μm.

but impaired the upper band (Fig. 6E, compare lane 9 with lane 1). These results indicate that ZNF536 interrupts RARα from binding to RARE, while ZNF536 itself binds to RARE.

To address whether the endogenous ZNF536 protein binds to RARE in the genome DNA, we performed a ChIP experiment. The results demonstrated that both the anti-ZNF536 antibodies and the anti-RARα antibody precipitated the RARE fragment (Fig. 6F), suggesting that both RARα and ZNF536 bind to the RARE fragment. Considering these results together with the results from EMSA, we propose that ZNF536 binds to RARE and affects RARα binding.

As RARα is one of the target genes induced by RA through RARE (16), we determined the expression levels of RARα in our stable cell lines. An RT-PCR analysis demonstrated that RA dramatically induced RARα expression in mock-transfected cells at 15 h but did not induce RARα expression in the ZNF536 stable expression cell line (Fig. 6G, lanes 2 and 6), suggesting that the overexpression of ZNF536 dramatically inhibits RARα expression. In a parallel experiment with a real-time RT-PCR analysis, we observed that overexpression of ZNF536 almost completely inhibited the expression of RARα in response to RA stimulation, whereas both the mu-

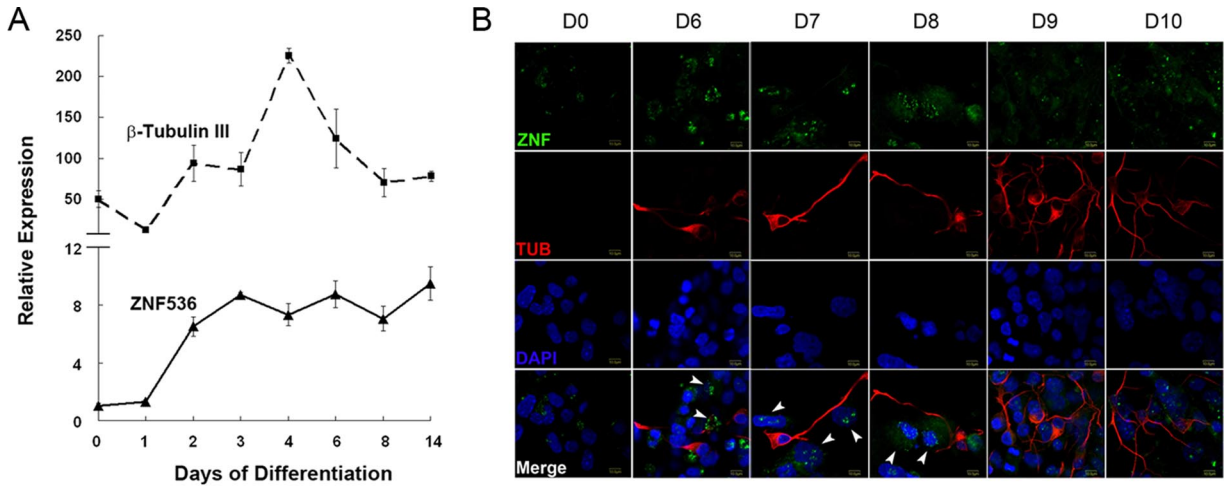


FIG. 4. Endogenous ZNF536 expression in RA-induced differentiated P19 EC cells. Endogenous ZNF536 and β-tubulin III expression in P19 cells in different phases of RA-induced differentiation are examined. (A) RNA was isolated from differentiated P19 cells on different days and subjected to real-time RT-PCR analysis. Expression of the indicated genes was analyzed in triplicate together with 18S rRNA. Results are presented as values relative to 18S, adjusted to the ZNF536 mRNA level of the undifferentiated sample, which was arbitrarily set to 1. (B) Expression of ZNF536 and the neuronal marker protein β-tubulin III during the differentiation process. An immunofluorescence assay was performed using antibodies as indicated. Day 0 (D0), wild-type P19 cells not induced; day 6 (D6) to day 10 (D10), differentiated P19 cells plating on tissue culture dishes after the suspension period. Cells with abundant expression of ZNF536 are indicated by arrows. Scale bars, 10 μm.

tation and the depletion of ZNF536 enhanced the basal level of RARα expression without RA stimulation (Fig. 6H). Interestingly, while mutant ZNF536 greatly enhanced RA-induced RARα expression, depletion of ZNF536 did not further increase RA-induced RARα expression. All of these results indicate that ZNF536 inhibits RA-induced RARα expression and that this inhibitory role is decreased by depletion or mutation of ZNF536.

**Rescue of RARα expression in ZNF536 stable cell lines restores RA-induced neuronal differentiation.** To test whether RARα affects the inhibitory role of ZNF536 on neuronal differentiation, we measured the effect of ectopically expressed human RARα on the inhibitory role of ZNF536 in transcriptional activity via the *RARE*-Luc reporter. The results show that overexpression of RARα stimulates reporter activity in mock-transfected cells and that this activity is inhibited by the

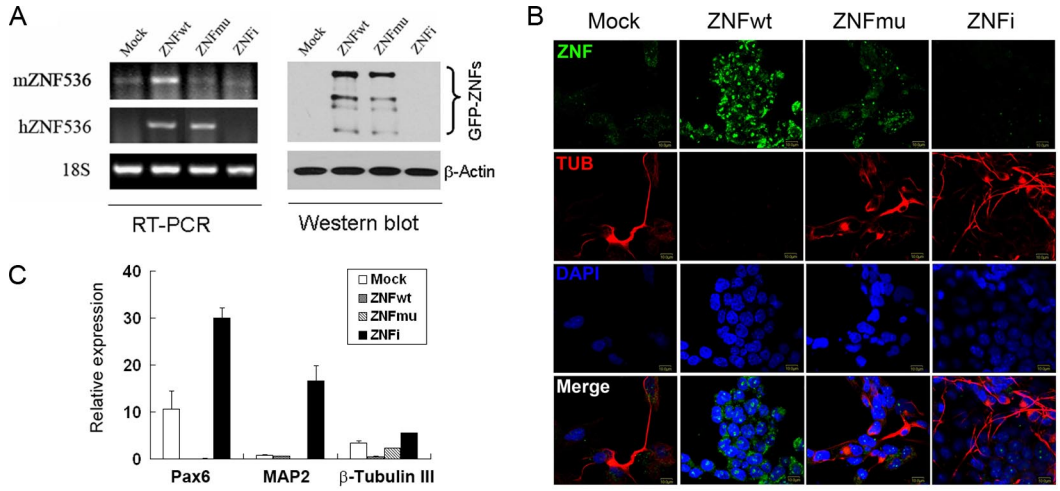


FIG. 5. Ectopic expression or depletion of ZNF536 influences P19 cell differentiation induced by RA. (A) Stable cell lines with overexpression or depletion of ZNF536 were selected based on P19 cells. Left, a semiquantitative RT-PCR was performed to confirm the levels of ZNF536. Mock-transfected (Mock), wild-type ZNF536 (ZNFwt), mutant ZNF536 (ZNFmu), and siRNA (ZNFi) stable cells are indicated. The primers were designed to specifically amplify mouse ZNF536 (mZNF536) and human ZNF536 (hZNF536). Right, a Western blot was performed to demonstrate the ectopically expressed Flag-ZNF536-GFP and Flag-ZNF536-GFP mutant proteins in the stable cell lines by an anti-GFP-antibody. (B) Expression of ZNF536 is inversely related to β-tubulin III levels. An immunofluorescence assay was formatted for the stable cell lines at 4 days after aggregation treatment with RA, using the antibodies indicated. Scale bars, 10 μm. (C) Overexpression or depletion of ZNF536 inhibits or enhances the expression of neuron marker genes. Real time RT-PCR analysis was performed for the stable cells at day 4 after aggregation treatment with RA. Each sample was analyzed in triplicate, and results are presented in arbitrary units relative to 18S, adjusted to the value for untreated (Mock) cells, which was set to 1.

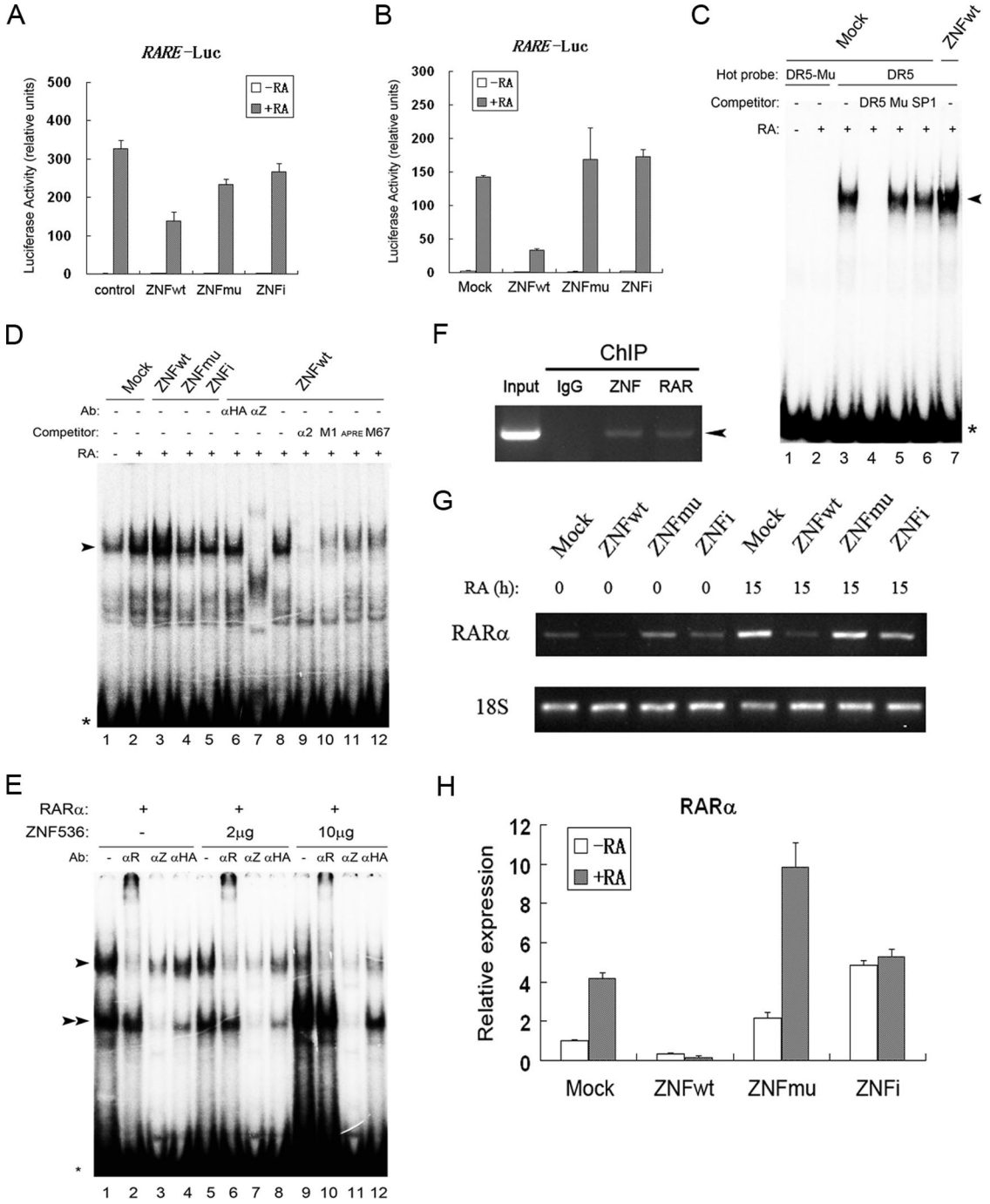


FIG. 6. ZNF536 inhibits RA-induced gene expression. (A) ZNF536 inhibits RA-stimulated *RARE*-Luc reporter activity. A luciferase assay was carried out using the *RARE*-Luc reporter. P19 cells were transfected with 200 ng *RARE*-Luc plasmid and 500 ng expression plasmids or control plasmid, as indicated, and then were treated with RA (+RA) or were left untreated (−RA). Results are the averages and SD from three independent experiments. (B) RA-induced luciferase reporter activation is inhibited by ZNF536 in the stable cells. A luciferase assay was carried out as in panel A, by using stable expressed P19 cell lines as indicated. Cells were transfected with *RARE*-Luc plasmid alone. (C) Ectopic expression of ZNF536 enhances the binding activity to classic RARE. $^{32}$P-labeled oligonucleotides containing a single RARE consensus sequence (DR-5) were incubated with the nuclear protein extracted from different stable cells (lane 3 to 7). The $^{32}$P-labeled mutant of DR-5 (DR-5Mu) was used as a negative control (lanes 1 and 2). Lanes 1 and 2, cell extracts from mock-transfected cells treated in the absence (−) or presence (+) of RA. The nuclear extracts used in lanes 3 to 6 are the same as those in lane 2. Lane 7, RA-treated cell extracts prepared from ZNFwt cells. Lanes 4 to 6, competition assay with nonradioactive (cold) specific probe DR-5, or DR-5Mu (Mu) and nonspecific probe SP1. Arrow shows the specific band. Asterisk shows free probe. (D) Ectopic expression of ZNF536 enhances the binding activity to RARα2-specific RARE. $^{32}$P-labeled oligonucleotides corresponding to the RARE sequence in the mouse RARα2 promoter (α2RARE) were incubated with nuclear protein extracted from different stable cells. Lanes 1 and 2, with cell extracts from mock-transfected cells treated in the absence (−) or presence (+) of RA. Lanes 3 to 5, with RA-treated cell extracts prepared from ZNFwt, ZNFmu and ZNFi cells, respectively. Lanes 6 and 7, supershift assay with nonspecific (αHA) or specific (αZ) antibody (Ab), respectively. Lanes 9 to 12, competition assay with cold specific probe α2RARE (α2) or mutant α2RARE

overexpression of ZNF536 (Fig. 7A), which is consistent with the results shown in Fig. 6.

We tested whether overexpression of RARα rescues the inhibitory role of ZNF536 in neuronal cell differentiation. We selected double stable cell lines that overexpress human RARα based on a stable cell line that overexpressed ZNF536 (Fig. 7B). A luciferase reporter assay indicated that overexpression of RARα rescued the inhibitory effect of ZNF536 on RA stimulation (Fig. 7C). A cell differentiation experiment showed that while ZNF536 dramatically inhibited the development of cells staining β-tubulin III positive, the overexpression of RARα restored RA-induced neuronal cell differentiation (Fig. 7D). These data imply that ZNF536 inhibits neuronal cell differentiation through RARα.

## DISCUSSION

Neurogenesis in the brains of adult mammals occurs throughout life. To date, emerging extrinsic factors and intracellular pathways have been implicated in regulating adult neuron stem cells and neural progenitors; however, the molecular mechanisms regulating adult neural progenitor differentiation remain unclear (38). In this study, we identified a novel zinc finger protein, ZNF536, as a negative regulator of neural cell differentiation. We found that expression of endogenous ZNF536 increases during the early stages of cell differentiation and remains at a constant high level in later stages but that overexpression of ZNF536 inhibits cell differentiation to neurons. As ZNF536 is specifically expressed in neuronal cells, we speculate that this gene plays an important role in the maintenance of neuronal cells. Our study reveals that ZNF536 is a negative regulator induced by RA during neuronal differentiation. This is very interesting, as most negative regulators of differentiation induced by RA in the nervous system are downregulated. For example, the tyrosine phosphatase protein SHP-1, which regulates the level of phosphorylation on the tyrosine residues of several intracellular proteins, is reduced in the late stages of neuronal differentiation (20). Our study implies that neuronal cells require not only positive regulators to promote cell differentiation but also negative regulators to inhibit cell differentiation during the entire process of neuron formation. This produces a scenario for cell differentiation with both positive and opposing effects. To our knowledge, this is the first zinc finger protein that acts as a negative regulator that is induced by RA during neuronal differentiation.

Our study also revealed that ZNF536 may function through RARα by binding to RARE in the promoters of downstream genes in the regulation of neuronal differentiation. Mouse RARα has two isoforms, mRARα1 and mRARα2. The expression of mRARα2 (in contrast to that of mRARα1) is induced by RA in EC F9 and P19 cells (15). Mouse RARα2 is transcribed from a promoter containing a RARE (16); therefore, RA induces RARα2 expression by enhancing RARα2 binding to RARE, generating positive feedback for the RA response during the upregulation of neuronal differentiation genes. In this study, we used a specific RARE from the mRARα2 promoter as a probe to demonstrate that ZNF536 enhances the binding ability of RARE in vitro and interrupts RAR binding to RARE, which results in the inhibition of transcription of RARα. We propose that ZNF536 functions in a negative feedback loop to regulate neuronal differentiation. Together with the observations that RARα is expressed during P19 cell differentiation and that overexpression of ZNF536 inhibits expression of RARα, we conclude that mRARα2 is downstream of ZNF536 in the regulation of neuronal differentiation. Our conclusion is further supported by the fact that hRARα1 (an orthologue of mRARα1 with a high level of identity to mRARα2) can restore ZNF536 overexpression of P19-stable cells to differentiate into neuron-like cells in response to RA.

P19 murine EC cells have been widely used for studies of in vitro neuronal differentiation. The sequential expression of neuronal surface markers, neurotransmitters, and their receptors in induced P19 cells resembles the processes observed during early in vivo development of neurons (33). P19 cells have been reported to survive and mature into functional neurons and glial cells when grafted into an adult rat striatum (22). RAC65 cells, mutant P19 cells containing a dominant negative form of RARα, abort neuronal maturation induced by RA, suggesting that RA induces P19 cell differentiation into neurons via RAR (1). In this study, we used P19 cells and observed that ZNF536 inhibits RARα transactivation and also interrupts the differentiation of P19 cells induced by RA. Our observations on the differentiation of P19 cells induced by RA are consistent with those in previous reports (33).

Zinc finger proteins form a large family of transcriptional regulators and can be subdivided into several subgroups

(M1) and STAT signal pathway-specific binding element (APRE and M67). The nuclear extracts used in lanes 6 to 12 are the same as those used in lane 3. Arrow shows the specific band. Asterisk shows free probe. (E) ZNF536 interrupts RARα binding to RARE while it binds to the element. $^{32}$P-labeled oligonucleotides containing DR-5 were incubated with the nuclear protein extracted from 293T cells transiently transfected with RARα and ZNF536 plasmids. Lanes 1 to 4, cell extracts from 293T cells transfected by RARα. Lanes 5 to 8, cell extracts from 293T cells transfected by RARα and 2 μg ZNF536. Lanes 9 to 12, cell extracts from 293T cells transfected by RARα and 10 μg ZNF536. Lanes 2, 6, and 10, supershift assay with anti-RARα antibody (αR). Lanes 3, 7, and 11, supershift assay with anti-ZNF536 antibody (αZ). Lanes 4, 8, and 12, supershift assay with nonspecific antibody (αHA). The single arrowhead shows the specific band of RARα complex. The double arrowheads show the specific band of the ZNF536 complex. Asterisk shows the free probe. (F) ZNF536 and RARα bind to the genome DNA of mouse RARE. A ChIP experiment was performed to demonstrate the endogenous protein binding to the RARE. Both anti-ZNF536 antibodies (ZNF) and anti-RARα antibody (RAR) were used. IgG was used as a negative control. (G) ZNF536 inhibits RA-induced RARα expression examined by semiquantitative RT-PCR. Different cell lines were treated with RA (0.3 μM) for 0 or 15 h prior to collecting as indicated. (H) A real-time PCR analysis demonstrates the inhibitory role of ZNF536 on RARα expression. RNA was prepared as in panel G. Each sample was analyzed in triplicate with 18S, and results are presented as the level of expression relative to 18S, adjusted to the value for untreated (Mock) cells, which was set to 1. ZNFwt, wild-type ZNF; ZNFmu, mutant ZNF536; ZNFi, ZNF536 siRNA; −RA, without RA; +RA, with RA.

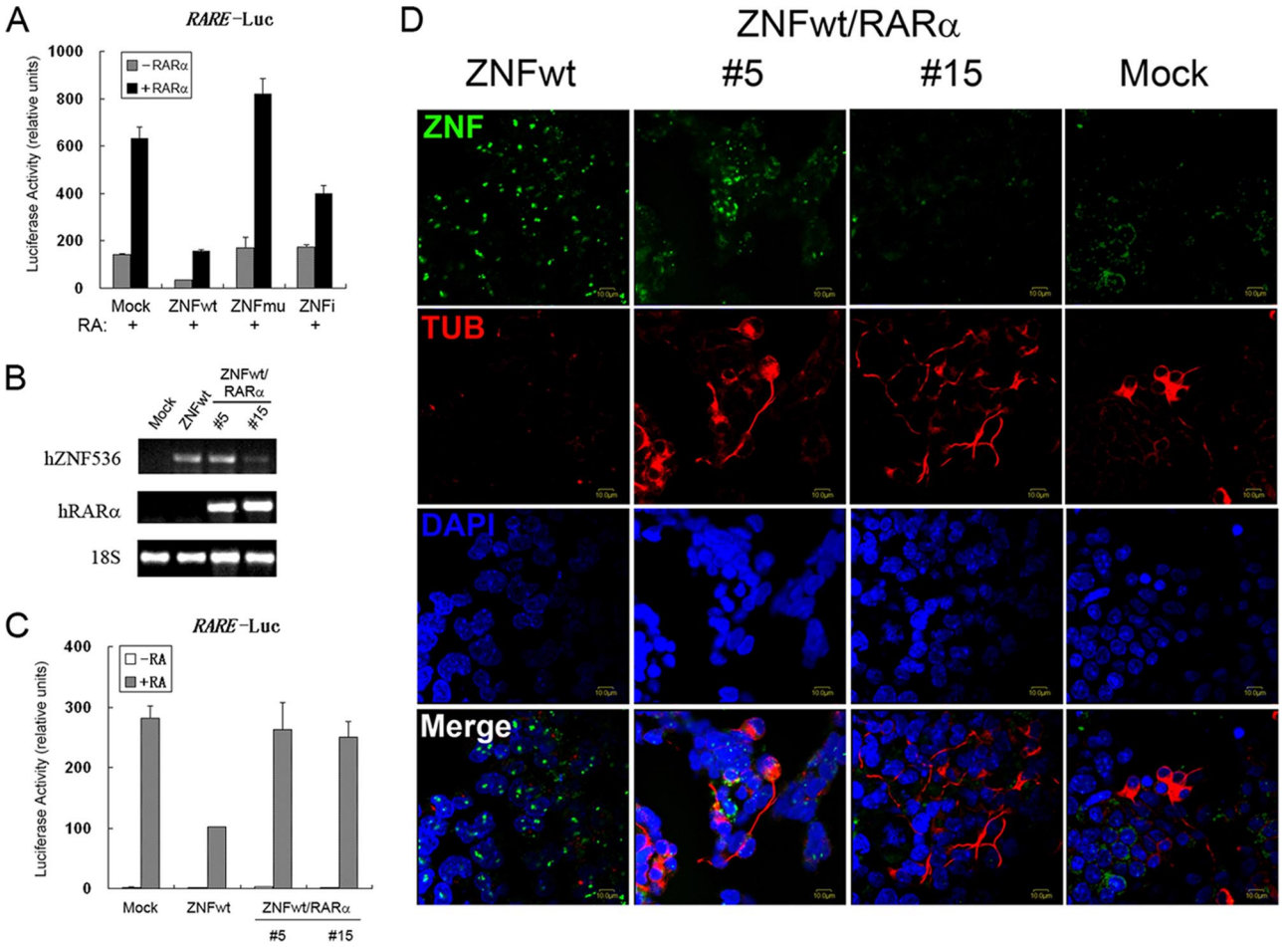


FIG. 7. Rescue of RARα expression in ZNF536 ectopically expressed stable cells restores RA-induced differentiation potential. (A) Overexpression of RARα enhances RA stimulated *RARE*-Luc reporter activity inhibited by ZNF536. Luciferase assay was carried out using stable expression P19 cell lines as indicated. Cells were transfected with (+RARα) or without (−RARα) 500 ng of RARα expression plasmid and treated with RA, together with expression of the *RARE*-Luc reporter. (B) Establishment of double overexpression cell lines for RARα and ZNF536. Cell lines (#5 and #15) were selected based on ZNF536 overexpression cell lines for RARα. A semiquantitative RT-PCR assay was performed to confirm ectopic expression of human RARα and ZNF536 in mock-transfected cells and in stable cells expressing wild-type ZNF536 (ZNFwt) and double ectopically expressing wild-type ZNF536/RARα. The primers were designed to specifically amplify human ZNF536 (hZNF536) and human RARα (hRARα). (C) Rescue of RARα expression in double overexpression stable cells restores luciferase reporter activity. Cells were transfected with the *RARE*-Luc plasmid and treated with RA (+RA) or left untreated (−RA). Results are presented as averages and SD from three independent experiments. (D) Overexpression of RARα rescues the inhibitory effect of ZNF536 (ZNF) on the expression of β-tubulin III (TUB). An immunofluorescence assay was performed using the stable cells at day 4 after aggregation treatment with RA. Scale bars, 10 μm.

based on the features of their zinc fingers and other motifs (7, 32). A sequence analysis shows that ZNF536 contains 10 Kruppel-like C2H2 zinc fingers and is highly conserved in vertebrates. It appears that ZNF536 does not belong to any of the known subfamilies of the Kruppel zinc fingers, as the highest similarity to the Kruppel zinc finger proteins is only 58% (to ZNF219), much lower than the similarities (86% to 100%) among orthologues of different species. Considering the expression patterns, we propose that ZNF536 represents a novel subfamily of brain-specific zinc finger protein different from other Kruppel-like zinc finger proteins (e.g., ZNF219, which exhibits ubiquitous expression in most fetal and adult tissues) (26).

Notably, ZNF536 contains a CtBP-binding motif. Interestingly, when we mutated this motif, we observed that ZNF536 lost its ability to inhibit both neuronal cell differentiation and RA-induced luciferase activity. These observations imply that the CtBP-binding motif is critical for the inhibitory role of ZNF536 in the regulation of RAR transcription. As corepressors of CtBPs also recruit RAR/RXR complexes in the regulation of target gene transcription (2), we speculate that CtBP may also play a role in the inhibition of RA-induced gene transcription, together with ZNF536. Additional studies are required to reveal the details of the mechanisms of the inhibitory role of ZNF536 in RA-induced gene expression during neuronal differentiation.

In conclusion, we have identified a novel zinc finger protein, ZNF536, which is expressed at high levels in the brains of both developing mouse embryos and adult mice. Our studies demonstrate that ZNF536 has a significant role in the regulation of RA-induced P19 cell differentiation by negatively regulating RARE-mediated downstream gene transcription.

## ACKNOWLEDGMENTS

This work was supported by Tsinghua-Yue-Yuan Medical Sciences Fund and grants from the National Natural Science Foundation of China (30530420, 30611120522) and the Chinese National Support Project (2006CB910102).

We are grateful to Yang Shi (Harvard Medical School), Xin-Yuan Fu (Indiana University School of Medicine), and Xiaofan Wang (Duke University) for their support and suggestions on this project. We thank Takahiro Nagase (KAZUSA DNA research institute, Japan) and Merlin Crossley (The University of Sydney, Australia) for providing constructs. We thank David M. Irvin (University of Toronto) for reading the manuscript.

## REFERENCES

1. **Bain, G., W. J. Ray, M. Yao, and D. I. Gottlieb.** 1994. From embryonal carcinoma cells to neurons: the P19 pathway. Bioessays **16:**343–348.
2. **Bartholin, L., S. E. Powers, T. A. Melhuish, S. Lasse, M. Weinstein, and D. Wotton.** 2006. TGIF inhibits retinoid signaling. Mol. Cell. Biol. **26:**990–1001.
3. **Bastien, J., and C. Rochette-Egly.** 2004. Nuclear retinoid receptors and the transcription of retinoid-target genes. Gene **328:**1–16.
4. **Chambon, P.** 1996. A decade of molecular biology of retinoic acid receptors. FASEB J. **10:**940–954.
5. **Chinnadurai, G.** 2002. CtBP, an unconventional transcriptional corepressor in development and oncogenesis. Mol. Cell **9:**213–224.
6. **Correia, K. M., and R. A. Conlon.** 2001. Whole-mount in situ hybridization to mouse embryos. Methods **23:**335–338.
7. **Dang, D. T., J. Pevsner, and V. W. Yang.** 2000. The biology of the mammalian Kruppel-like family of transcription factors. Int. J. Biochem. Cell Biol. **32:**1103–1121.
8. **Duan, X., J. H. Chang, S. Ge, R. L. Faulkner, J. Y. Kim, Y. Kitabatake, X. B. Liu, C. H. Yang, J. D. Jordan, D. K. Ma, C. Y. Liu, S. Ganesan, H. J. Cheng, G. L. Ming, B. Lu, and H. Song.** 2007. Disrupted-In-Schizophrenia 1 regulates integration of newly generated neurons in the adult brain. Cell **130:** 1146–1158.
9. **Fode, C., Q. Ma, S. Casarosa, S. L. Ang, D. J. Anderson, and F. Guillemot.** 2000. A role for neural determination genes in specifying the dorsoventral identity of telencephalic neurons. Genes Dev. **14:**67–80.
10. **Glass, C. K., and M. G. Rosenfeld.** 2000. The coregulator exchange in transcriptional functions of nuclear receptors. Genes Dev. **14:**121–141.
11. **Guillemot, F., Z. Molnar, V. Tarabykin, and A. Stoykova.** 2006. Molecular mechanisms of cortical differentiation. Eur. J. Neurosci. **23:**857–868.
12. **Inoue, T., M. Ogawa, K. Mikoshiba, and J. Aruga.** 2008. *Zic* deficiency in the cortical marginal zone and meninges results in cortical lamination defects resembling those in type II lissencephaly. J. Neurosci. **28:**4712–4725.
13. **Jones-Villeneuve, E. M., M. W. McBurney, K. A. Rogers, and V. I. Kalnins.** 1982. Retinoic acid induces embryonal carcinoma cells to differentiate into neurons and glial cells. J. Cell Biol. **94:**253–262.
14. **Kiehl, T. R., S. E. Fischer, S. Ezzat, and S. L. Asa.** 2008. Mice lacking the transcription factor Ikaros display behavioral alterations of an anti-depressive phenotype. Exp. Neurol. **211:**107–114.
15. **Leroy, P., A. Krust, A. Zelent, C. Mendelsohn, J. M. Garnier, P. Kastner, A. Dierich, and P. Chambon.** 1991. Multiple isoforms of the mouse retinoic acid receptor alpha are generated by alternative splicing and differential induction by retinoic acid. EMBO J. **10:**59–69.
16. **Leroy, P., H. Nakshatri, and P. Chambon.** 1991. Mouse retinoic acid receptor alpha 2 isoform is transcribed from a promoter that contains a retinoic acid response element. Proc. Natl. Acad. Sci. USA **88:**10138–10142.
17. **Li, L. Y., H. Xin, X. L. Xu, M. Huang, X. J. Zhang, Y. Chen, S. P. Zhang, X. Y. Fu, and Z. J. Chang.** 2004. CHIP mediates degradation of Smad proteins and potentially regulates Smad-induced transcription. Mol. Cell. Biol. **24:**856–864.
18. **Maden, M.** 2007. Retinoic acid in the development, regeneration and maintenance of the nervous system. Nat. Rev. Neurosci. **8:**755–765.
19. **Maden, M.** 2001. Role and distribution of retinoic acid during CNS development. Int. Rev. Cytol. **209:**1–77.
20. **Mizuno, K., T. Katagiri, E. Maruyama, K. Hasegawa, M. Ogimoto, and H. Yakura.** 1997. SHP-1 is involved in neuronal differentiation of P19 embryonic carcinoma cells. FEBS Lett. **417:**6–12.
21. **Molofsky, A. V., S. He, M. Bydon, S. J. Morrison, and R. Pardal.** 2005. Bmi-1 promotes neural stem cell self-renewal and neural development but not mouse growth and survival by repressing the p16Ink4a and p19Arf senescence pathways. Genes Dev. **19:**1432–1437.
22. **Morassutti, D. J., W. A. Staines, D. S. Magnuson, K. C. Marshall, and M. W. McBurney.** 1994. Murine embryonal carcinoma-derived neurons survive and mature following transplantation into adult rat striatum. Neuroscience **58:** 753–763.
23. **Quinlan, K. G., M. Nardini, A. Verger, P. Francescato, P. Yaswen, D. Corda, M. Bolognesi, and M. Crossley.** 2006. Specific recognition of ZNF217 and other zinc finger proteins at a surface groove of C-terminal binding proteins. Mol. Cell. Biol. **26:**8159–8172.
24. **Rastinejad, F.** 2001. Retinoid X receptor and its partners in the nuclear receptor family. Curr. Opin. Struct. Biol. **11:**33–38.
25. **Sakai, T., K. Hino, S. Wada, and H. Maeda.** 2003. Identification of the DNA binding specificity of the human ZNF219 protein and its function as a transcriptional repressor. DNA Res. **10:**155–165.
26. **Sakai, T., A. Toyoda, K. Hashimoto, and H. Maeda.** 2000. Isolation and characterization of a novel zinc finger gene, ZNF219, and mapping to the human chromosome 14q11 region. DNA Res. **7:**137–141.
27. **Shi, Y., D. Chichung Lie, P. Taupin, K. Nakashima, J. Ray, R. T. Yu, F. H. Gage, and R. M. Evans.** 2004. Expression and function of orphan nuclear receptor TLX in adult neural stem cells. Nature **427:**78–83.
28. **Sidell, N., A. Altman, M. R. Haussler, and R. C. Seeger.** 1983. Effects of retinoic acid (RA) on the growth and phenotypic expression of several human neuroblastoma cell lines. Exp. Cell Res. **148:**21–30.
29. **Simpson, T. I., and D. J. Price.** 2002. Pax6; a pleiotropic player in development. Bioessays **24:**1041–1051.
30. **Song, J., Y. C. Lu, K. Yokoyama, J. Rossi, and R. Chiu.** 2004. Cyclophilin A is required for retinoic acid-induced neuronal differentiation in p19 cells. J. Biol. Chem. **279:**24414–24419.
31. **Sun, G., R. T. Yu, R. M. Evans, and Y. Shi.** 2007. Orphan nuclear receptor TLX recruits histone deacetylases to repress transcription and regulate neural stem cell proliferation. Proc. Natl. Acad. Sci. USA **104:**15282–15287.
32. **Turner, J., and M. Crossley.** 1999. Mammalian Kruppel-like transcription factors: more than just a pretty finger. Trends Biochem. Sci. **24:**236–241.
33. **Ulrich, H., and P. Majumder.** 2006. Neurotransmitter receptor expression and activity during neuronal differentiation of embryonal carcinoma and stem cells: from basic research towards clinical applications. Cell Prolif. **39:**281–300.
34. **Xie, B., J. Zhao, M. Kitagawa, J. Durbin, J. A. Madri, J. L. Guan, and X. Y. Fu.** 2001. Focal adhesion kinase activates Stat1 in integrin-mediated cell migration and adhesion. J. Biol. Chem. **276:**19512–19523.
35. **Yang, V. W.** 1998. Eukaryotic transcription factors: Identification, characterization and functions. J. Nutr. **128:**2045–2051.
36. **Zetterstr ö m, R. H., E. Lindqvist, A. Mata de Urquiza, A. Tomac, U. Eriksson, T. Perlmann, and L. Olson.** 1999. Role of retinoids in the CNS: differential expression of retinoid binding proteins and receptors and evidence for presence of retinoic acid. Eur. J. Neurosci. **11:**407–416.
37. **Zhang, Y. J., T. S. Li, L. Fu, C. M. Yu, Y. H. Li, X. L. Xu, Y. Y. Wang, H. X. Ning, S. P. Zhang, W. Chen, L. A. Babiuk, and Z. J. Chang.** 2004. Silencing SARS-CoV Spike protein expression in cultured cells by RNA interference. FEBS Lett. **560:**141–146.
38. **Zhao, C., W. Deng, and F. H. Gage.** 2008. Mechanisms and functional implications of adult neurogenesis. Cell **132:**645–660.